IEEE Access
Multidisciplinary | Rapid Review | Open Access Journal

Received December 20, 2018, accepted January 7, 2019, date of publication January 11, 2019, date of current version February 4, 2019.

Digital Object Identifier 10.1109/ACCESS.2019.2892559

Underdetermined Source Separation of Bearing Faults Based on Optimized Intrinsic Characteristic-Scale Decomposition and Local Non-Negative Matrix Factorization

YANSONG HAO[1], LIUYANG SONG[1], MENGYANG WANG[1], LINGLI CUI[2], (Member, IEEE), AND HUAQING WANG[1], (Member, IEEE)

[1]College of Mechanical and Electrical Engineering, Beijing University of Chemical Technology, Beijing 100029, China
[2]Beijing Engineering Research Center of Precision Measurement Technology and Instruments, Beijing University of Technology, Beijing 100124, China

Corresponding authors: Lingli Cui (acuilingli@163.com) and Huaqing Wang (hqwang@mail.buct.edu.cn)

This work was supported by the National Natural Science Foundation of China under Grant 51675035, Grant 51575007, and Grant 51805022.

ABSTRACT Since roller bearing is one of the most vulnerable components, bearing faults usually occur in an unprepared situation with multiple faults, and the quantity of sensors is limited in the real-time working environment, resulting in an underdetermined blind source separation (UBSS) problem to extract the fault features. Because the collected signals are usually not independent and not sparse enough, traditional methods of separating signals cannot perform well. In this paper, an optimized intrinsic characteristic-scale decomposition (OICD) method is proposed to solve the underdetermined problem. Meanwhile, the constraint error factor is introduced to overcome the drawback that the ideal ending condition of ICD is not proper for the vibration signal of bearing. In addition, given that non-negative matrix factorization (NMF) is not limited by the source signal independence and sparsity, an improved UBSS model is constructed, and the PCs are used as the input matrix of local NMF to obtain the separation signal. Ultimately, envelope analysis is utilized to detect the source signal feature. Both simulated and experimental vibration signals are used to verify the effectiveness of the proposed approach. Besides, the traditional method is juxtaposed with the suggested method. The results indicate that the proposed method is effective in dealing with the compound faults separation of the rotating machinery.

INDEX TERMS Local non-negative matrix factorization, underdetermined blind source separation, optimized intrinsic characteristic-scale decomposition.

I. INTRODUCTION

Rotating machinery, particularly roller bearing, is of great importance to the industries and enterprise. Since roller bearing is one of the most vulnerable components, bearing faults usually occur in an unprepared situation, resulting in a large amount of maintenance costs and economic losses [1], [2]. Moreover, owing to complex working conditions, roller bearing failure is often accompanied by multiple component faults. To ensure that the bearing is operated under healthy conditions, it is essential to carry out the compound faults diagnosis [3]–[6]. Many different techniques, such as vibration, force, and temperature, have been developed for rotating machinery fault diagnosis. On account of its convenience in measurement and analysis of vibration signal, it has been extensively utilized in condition monitoring and fault diagnosis of rotating machine [7]–[10].

There are many proposed analysis methods based on vibration signal. For instance, Islam *et al.* [11] proposed a fault analysis method to maximize incipient fault features based on computed order tracking with adaptive filter and cyclic logarithmic envelope spectrum, which can effectively strengthen the early failure signatures of rotating machines. Yan *et al.* [12] suggested a novel Time-Frequency Representation (TFR) approach based on Frequency Slice Wavelet Transform (FSWT). Although these methods perform well in bearing diagnosis, they cannot work well when compound

faults occur owing to the interaction between multiple fault source signals and the complexity of the transmission path of the vibration signal. Therefore, achieving the separation of compound faults is presently a hot spot for scholars.

Aiming to obtain the source signal from the mixed signal, BSS (blind source separation) —- which contains ICA, sparse component analysis (SCA), and non-negative matrix factorization (NMF) —- was proposed to achieve the process [13]–[15]. Many investigators proposed approaches based on ICA to detect the feature when the information of observation is sufficient. For example, Spurek *et al.* [16] presented a method to ICA based on the split Gaussian distribution, which is well adapted to asymmetric data. Wang et al. introduced ICA into the EMD procedure to make the components orthogonal to one another, cutting down the redundancy of the components [17]. In addition, SCA was developed in recent years and utilizes the sparsity to separate the signal. Amini and Hedayati [18] and Xu *et al.* [19] advised a novel blind modal identification approach that can identify the modal parameters of structures. NMF is a new matrix decomposition algorithm. Since it was first presented by scientists of Lee and Seung in 1999, this decomposition algorithm has been accepted and applied to various fields [20]–[22]. Canadas-Quesada *et al.* [23] proposed a non-negative matrix factorization approach to extract heart sounds from mixtures composed of heart and lung sounds. In fact, sensors for data collection of rotating machinery typically need to be installed in a limited number of specific locations, and in most cases the quantity of fault sources exceeds the quantity of observed signals. Therefore, extracting the faults features from the observed signals is to solve an UBSS issue actually and previous research on ICA failed to consider this case [24]. To overcome the underdetermined problem when ICA is utilized, Wang *et al.* [25] presented an effective fault component separation method that integrates ensemble empirical mode decomposition (EEMD) with ICA, without requiring a priori information on the rotating speeds or bandwidth. Wang *et al.* [26] proposed a BSS method based on EEMD and ICA, and the compound faults were successfully separated according to this method. Hao *et al.* [27] presented a sparsity-based SCA method which can improve the sparsity of mixed signal before estimating the matrix. These methods have acquired great improvement. Nevertheless, some drawbacks still exist. ICA requires source signals to be independent of each other, which is difficult to meet in actual industrial production. Besides, although SCA can separate the source signal according to the sparsity, the sparsity for vibration signals is always unsatisfactory due to the complex condition.

Therefore, considering the logic of ICA in solving UBSS and NMF has no strict qualifications on the source signal, a framework is constructed to deal with UBSS problem in this paper. ICD method is a new adaptive time-frequency analysis method [28]. In this framework, an optimized ICD algorithm is utilized to obtain more observed channels to address the deficiency of sensors and solve the underdetermined BSS problem. A constraint error factor (CEF) is introduced to optimize the problem that the strict convergence condition of ICD not being applicable to the faulty bearing. Furthermore, potential function is used to estimate the source signal quantity. Last, considering LNMF is a procedure which can impose the locality of features in basis components and to make the representation suitable for tasks, LNMF is utilized in this paper. Multiple channels are accordingly constituted input matrix of LNMF algorithm to obtain separated signal.

The remaining sections are organized as follows. Section II describes the process of optimizing ICD method. The specific technique of compound faults separation based on the suggested method is presented in Section III. The investigation of simulated signals and experimental signals are discussed in Section IV. Finally, the results are summarized in Section V.

II. ELIMINATE UNDERDETERMINED CONSTRAINTS IN UBSS

A. UBSS STATEMENT

The main task of BSS is to separate source signals from the acquired observed signals if the source signal and the transmission channel are unknown. Its ideal model can be presented as:

$$X(t) = AS(t) \tag{1}$$

where $S(t) = [S_1(t), S_2(t), \ldots, S_n(t)]^T$ represents the source signal; A means a mixed matrix; $X(t) = [X_1(t), X_2(t), \ldots, X_m(t)]^T$ on behalf of the observation signal. When $m < n$, the BSS is an UBSS issue. Drawing on the ideas of EEMD-ICA method mentioned in Section I, we use OICD to convert UBSS issue to BSS case.

B. OPTIMIZED INTRINSIC CHARACTERISTIC-SCALE DECOMPOSITION

ICD method is a new adaptive time-frequency analysis method that can decompose the original signal into several PCs. The decomposed processing can be expressed as follows.

$$x(t) = \sum_{i=1}^{n} PC_i(t) + r_n(t) \tag{2}$$

where PC is a component signal that is the product of a frequency modulated signal and an envelope signal, and $r_n(t)$ is the redundancy part of signal. A demodulation component $s_{1n}(t)$ will be generated during the iteration of processing. The ideal iteration termination condition is that the $s_{1n}(t)$ is a purely frequency signal. However, vibration signals mixed strong noise in actual industrial condition, which may result in the ICD algorithm not converge based on the ideal termination criterion. Therefore, a constraint error factor (CEF) is introduced to optimize the algorithm with complex vibration signal. One approach is to allow little error points exist because these points will never satisfy the terminal principle as the number of iterations increases. Therefore, we set a CEF

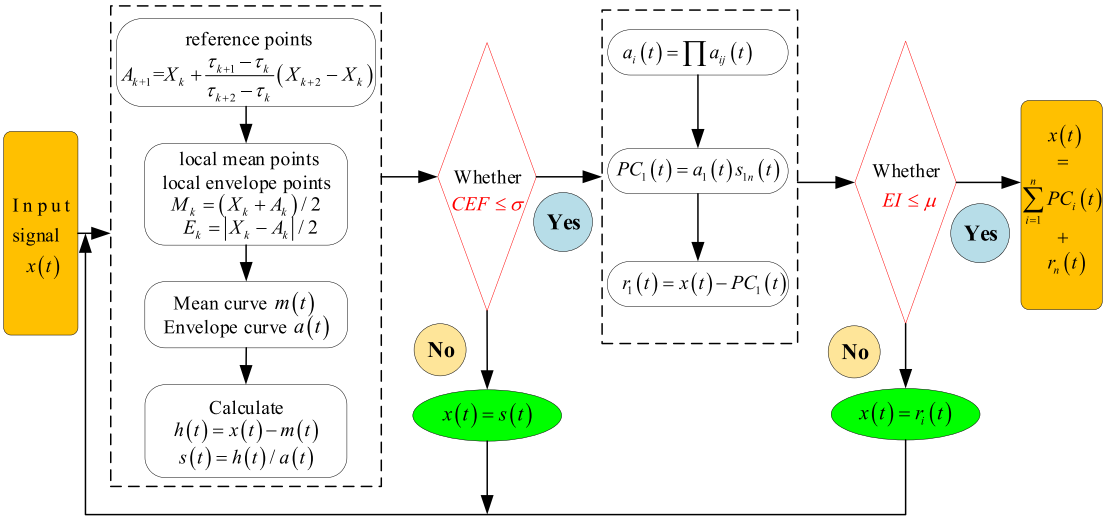

FIGURE 1. The flowchart of optimized ICD algorithm.

to avoid the algorithm non convergence.

$$CEF = N\left(s'\left(t\right)\right)/N\left(x\left(t\right)\right) \tag{3}$$

where $N\left(s'\left(t\right)\right)$ is the length of sample points $s'\left(t\right)$ that do not satisfy $-1 \leq s_{1n}\left(t\right) \leq 1$, and $N\left(x\left(t\right)\right)$ is the length of original signal $x\left(t\right)$. In addition, an energy index (EI) is used as the reference of PCs, which can improve the efficiency of the algorithm.

$$EI = \frac{\left\|x\left(t\right)\right\|_2^2 - \left\|\sum_{i=1}^{n-1} PC\left(t\right)_i\right\|_2^2}{\left\|\sum_{i=1}^{n} PC\left(t\right)_i\right\|_2^2} - \frac{\left\|x\left(t\right)\right\|_2^2 - \left\|\sum_{i=1}^{n} PC\left(t\right)_i\right\|_2^2}{\left\|\sum_{i=1}^{n} PC\left(t\right)_i\right\|_2^2} \tag{4}$$

For a given signal $x\left(t\right)$, the specific procedures of OICD are introduced as follows.

Step 1: Obtain the reference points A_k.

Step 2: Calculate the local mean points and local envelope points.

Step 3: Sever the mean curve $m_1\left(t\right)$ and then demodulate to get $s_{11}\left(t\right)$.

Step 4: Repeat steps 1-3 until CEF condition is satisfied.

Step 5: Acquire the first $PC_1\left(t\right)$.

Step 6: Separate $PC_1\left(t\right)$ from the original signal to obtain the remaining part $r_1\left(t\right)$ and regard $r_1\left(t\right)$ as the original data, then continue to repeat the above steps m times until the PCs number equals to the source number.

The details are shown in Fig. 1.

III. COMPOUND FAULTS SIGNAL SEPARATION

A. NON-NEGATIVE MATRIX FACTORIZATION

The model of non-negative matrix factorization can be simply described as follows: given a non-negative matrix $V = \left(v_1, \ldots, v_n\right) \in R_+^{m\times n}$, and the non-negative matrix V can be factorized by a product of two non-negative matrices $W \in R_+^{m\times r}$ and $H \in R_+^{r\times n}$ as well as possible, namely

$$V_{m\times n} \approx W_{m\times r} H_{r\times n} \tag{5}$$

where $V_{m\times n}$ denotes a matrix with the dimension of m whereas n represents the number of samples. $W_{m\times r}$ is a basis matrix which can be regarded as a series of basis vectors. $H_{r\times n}$ is a coefficient matrix which can be regarded as the coordinates of each samples with respect to these basis vectors. The principle of NMF algorithm is shown in Fig. 2.

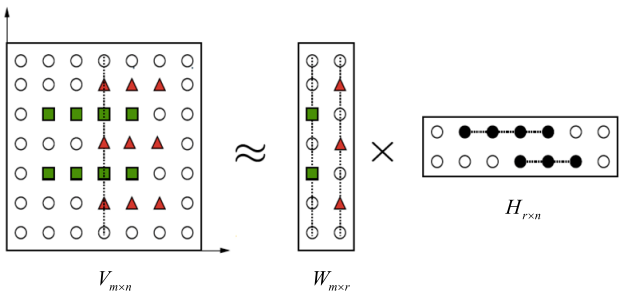

FIGURE 2. The principle of NMF algorithm.

Since the NMF algorithm has been proposed, a variety of cost function to optimize the NMF algorithm is used. Traditionally, the cost function is based on the square of the norm:

$$D\left(V\|WH\right) = \|V - WH\|^2 \quad s.t.\ W, \quad H > 0 \tag{6}$$

The NMF algorithm with the cost function of (6) is defined as the following optimization problem:

$$\min \|V - WH\|^2 = \sum_{ij} [v_{ij} - (WH)_{ij}]^2 \tag{7}$$

The optimization problem in (7) is convex to W and H, respectively. However, it is nonconvex when the factors W and H exist simultaneously. The above optimization problem can be solved by multiplicative updated algorithms, alternating and iterating until convergence. The updated rules are determined by

$$w_{ik} \leftarrow w_{ik} \frac{(VH^T)_{ik}}{(WHH^T)_{ik}} \quad h_{ik} \leftarrow h_{ik} \sum_i \frac{(W^T V)_{kj}}{(W^T WH)_{kj}} \tag{8}$$

Later, the objective function is constructed for preventing Poisson noise as

$$\begin{aligned} &\min\ D(V\|WH) = \sum_{ij} [v_{ij} \log \frac{v_{ij}}{(WH)_{ij}} - v_{ij} + (WH)_{ij}] \\ &s.t.\ W, H > 0 \end{aligned} \tag{9}$$

where the update criteria are shown as

$$w_{ik} \leftarrow w_{ik} \frac{\sum_j \frac{h_{kj} v_{ij}}{(WH)_{ij}}}{\sum_u h_{ku}} \ h_{kj} \leftarrow h_{kj} \frac{\sum_i \frac{w_{ik} v_{ij}}{(WH)_{ij}}}{\sum_v w_{vk}} \tag{10}$$

B. LOCAL NON-NEGATIVE MATRIX FACTORIZATION

The method of LNMF is proposed on the basis of traditional NMF. It is initially applied in the field of image processing, which can make the local features more obvious, and has been successfully applied in face recognition. The LNMF algorithm is based on the KL divergence model, which imposes a basis orthogonality constraint on its objective function, reducing the redundancy between the base vectors. Random matrix is used as the initialization condition of the algorithm.

The objective function of LNMF algorithm can be defined as follows:

$$\begin{aligned} D(V\|WH) = \sum_{i,j} [V_{ij} \lg \frac{V_{ij}}{(WH)_{ij}} - V_{ij} + (WH)_{ij}] \\ +\alpha \sum_{ij} (u_{ij}) - \beta \sum_i (v_{ii}) \end{aligned} \tag{11}$$

where $[u_{ij}] = U = W^T W$, $[v_{ij}] = V = HH^T$, $\alpha, \beta \in R_+$.

The LNMF algorithm mainly imposes three constraints on the objective function:

(1) Calculate $\min \sum_{i \neq j} u_{ij}$ to keep the base matrix W as orthogonal as possible to reduce redundancy between the base vectors.

(2) Calculate $\min \sum_i u_{ii}$ to maximize the sparsity of the coefficient matrix H in order to generate more local features.

(3) Calculate $\max\ v_{ii}$ to make the base vector from the largest representative.

The iterative formula for W_{ij} and H_{ji} are listed as follows

$$W_{ij} = (W_{ii} \sum_i v_{ii} \frac{H_{ji}}{\sum_i W_{ii} H_{ji}}) / \sum_i H_{ji} \tag{12}$$

$$W_{ij} = W_{ij} / \sum_{ij} W_{ij} \tag{13}$$

$$H_{ji} = \sqrt{(H_{ji} \sum_i v_{ii} \frac{W_{ij}}{\sum_j W_{ii} H_{ji}})} \tag{14}$$

C. ESTIMATE THE QUANTITY OF SOURCES USING POTENTIAL FUNCTION

The PCs number have been determined based on the EI, which means the m has been determined. To definite the r in LNMF, potential function is used to estimate the output of the algorithm.

$$\Phi(\theta, \lambda) = \sum_t r_t \gamma(\lambda(\theta - \theta_t)) \tag{15}$$

where λ is a constant that can impact the effect of the α. The larger the value of λ, the higher the resolution of the function, whereas the smaller the value of λ, the lower the resolution of the function. Usually its value is 5. In two-dimension case, $r_t = \sqrt{x_1^2(t) + x_2^2(t)}$ and $\theta_t = \tan^{-1}(x_2(t)/x_1(t))$. The value of the function γ is as follows

$$\gamma(\alpha) = \begin{cases} 1 & -\frac{\alpha}{\pi/4} \ |\alpha| < \pi/4 \\ 0 & \text{elsewhere} \end{cases} \tag{16}$$

When the column vector of the mixing matrix is just at the actual observation signal θ_k, the potential function $\Phi(\theta_k)$ calculated by the column vector at this time takes the maximum value. Therefore, the number of local maxima in the potential function graph is equal to the number of column vectors of the mixing matrix, that is, the number of source signals.

D. THE SUGGESTED DIAGNOSIS TECHNIQUE

After the quantity of source have been estimated, the dimension of the W and H are determined. Therefore, although the number of observed signals is insufficient, we solved the underdetermination of UBSS by OICD decomposition. And by estimating the number of source signals, the number of LNMF outputs is completely determined. The compound faults diagnosis framework overcomes the dependence of traditional methods on source signal independence and sparsity. Details of the diagnosis framework is presented in Fig. 3.

IV. THE SIMULATION AND EXPERIMENT

A. SIMULATION ANALYSIS

Simulation is constructed to verify the effectiveness of the proposed method. According to (17), two single simulated signals are used as the experimental subject, and their characteristic frequencies are $f_1 = 15Hz$ and $f_2 = 35Hz$, respectively. The spectra of source signal are presented in Fig. 4. According to (18), the two signals are randomly mixed

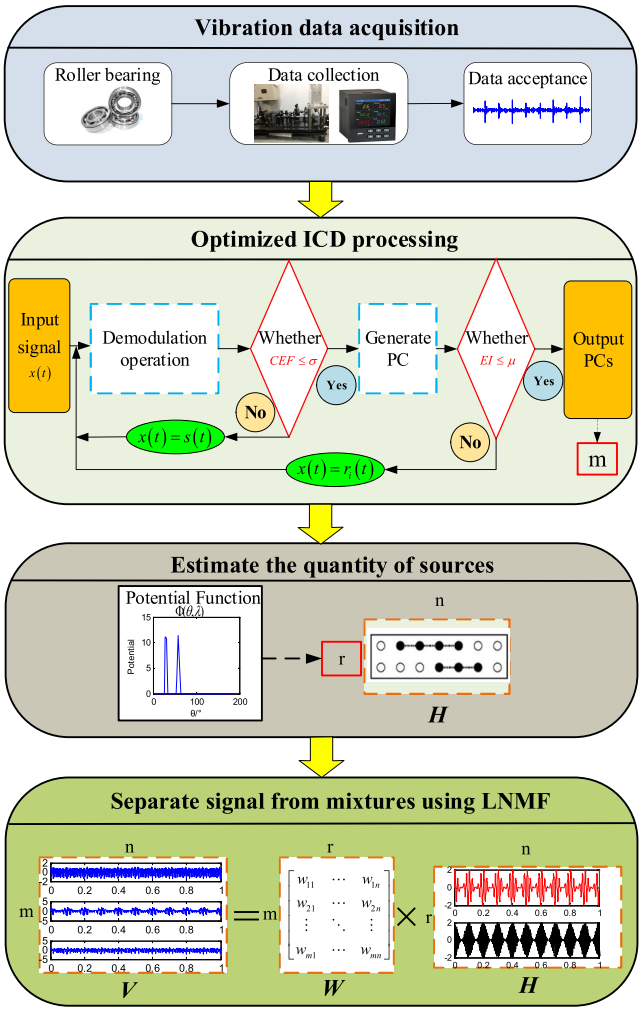

FIGURE 3. The flowchart of proposed method.

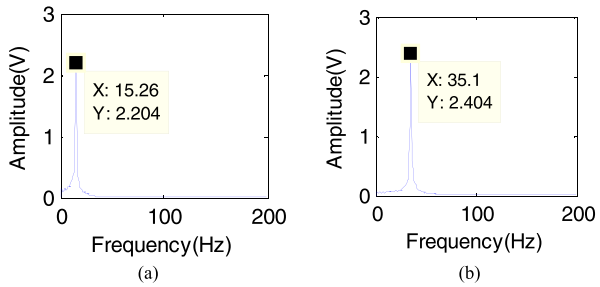

FIGURE 4. Spectra of source signals: (a) spectrum of s_1; (b) spectrum of s_2.

into one observed signal. In addition, the mixed matrix is $A = [0.8147\ 0.9058]$. The spectrum of mixed signal is shown in Fig. 5 and the source features cannot be separated. Therefore, the next diagnosis approach according to the process shown in Fig. 3 is adopted. First, we use the single-column channel of the mixed signal for OICD decomposition according to the technical route mentioned above. In this occasion, two PCs are obtained which indicates the row quantity m of

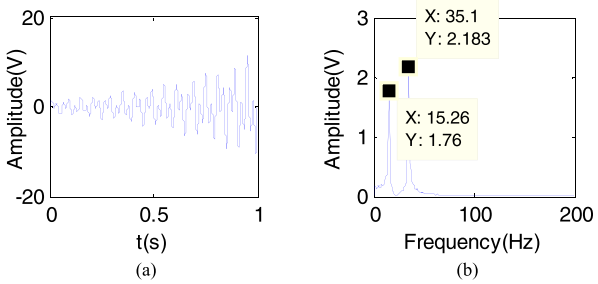

FIGURE 5. The mixed signal: (a) The waveform of the mixed signal; (b) The spectrum of the mixed signal.

the matrix V and W in the LNMF. Second, the two PCs are used to reckon the quantity of source signal. Here, potential function is utilized to determine the quantity information buried in the mixtures. Fig. 6 presents the potential function $\Phi(\theta, \lambda)$ of mixtures, indicating that the quantity of sources is two based on the two peak points existed in the curve.

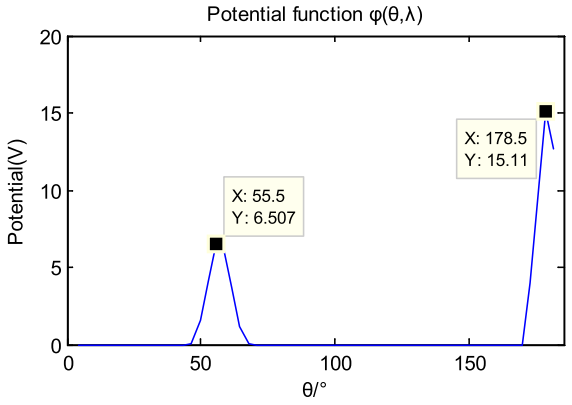

FIGURE 6. The potential function $\Phi(\theta, \lambda)$ of simulated mixtures.

In this step, the columns quantity r of W and H has been obtained. Ultimately, the source signal can be separated from the PCs and the result are included in the matrix H. The results presented in Fig. 7 indicates that the two original source signals are separated, proving the effectiveness of the proposed method.

$$\begin{cases} s_1 = e^{(2t)} \sin(2\pi f_1 t) \\ s_2 = e^{(2t)} \sin(2\pi f_2 t) \end{cases} \tag{17}$$

$$x(t) = As(t) = A[s_1(t), s_2(t)]^T \tag{18}$$

B. EXPERIMENTAL VERIFICATION

The simulation test bench of ball bearing fault diagnosis is utilized to confirm the availability of the method presented in the Section III. The simulation test setup is shown in Fig. 8, driven by a motor. In order to simulate the composite failure of the outer race and the rolling element, the corresponding part of the bearing is machined with a small defect. Accelerometer sensors installed on the bearing housing are used to acquire the vibration signals. Given that the fault

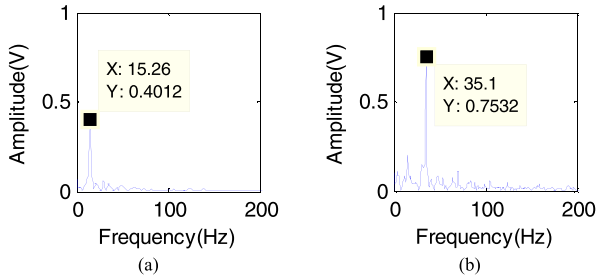

FIGURE 7. The separated signal: (a) The spectrum of s_1; (b) The spectrum of s_2.

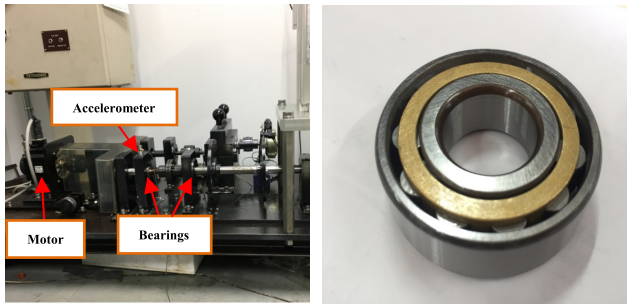

FIGURE 8. The experimental system. (a) Experimental table; (b) NTN N204 bearing.

TABLE 1. Structure Parameters of NTN N204 Bearing.

Number of Rollers	External Diameter (mm)	Inner Diameter (mm)	Width (mm)
10	47	20	14

features are apparent in the vertical direction, vertical sensor collects the signal utilized in this paper. NTN N204 bearing is used in the experiment and its structural parameters can be found in Table 1. Furthermore, the vibration signals collected at 900 rpm are utilized to verify the effectiveness of the proposed method.

$$f_o = \frac{Z}{2}(1 - \frac{d}{D}\cos\alpha)f_r \tag{19}$$

$$f_b = \frac{D}{2d}[1-(\frac{d}{D}\cos\alpha)^2]f_r \tag{20}$$

$$f_c = \frac{1}{2}[1-\frac{d}{D}\cos\alpha]f_r \tag{21}$$

The fault passing frequency of each element can be calculated according to (19-21). Where D represses the pitch diameter, Z represses the roller quantity, d represses the roller diameter, α is the roller contact angle, and f_r is the rotating frequency. f_o, f_b, and f_c are the fault characteristic frequencies of the outer race, rollers, and the cage. The estimated results based on the equations are presented in Table 2.

A Time-domain of vibration signal collected by a sensor and its spectrum are displayed in Fig. 9. As can be seen from the time domain waveform diagram, the bearing signal has mangy significant impact components, indicating that the

TABLE 2. Fault characteristic frequency of the roller bearings at 900 rpm.

Fault Location	Fault Characteristic Frequency
Outer race	60.5 Hz
Roller	74.4 Hz
Cage	6.0 Hz

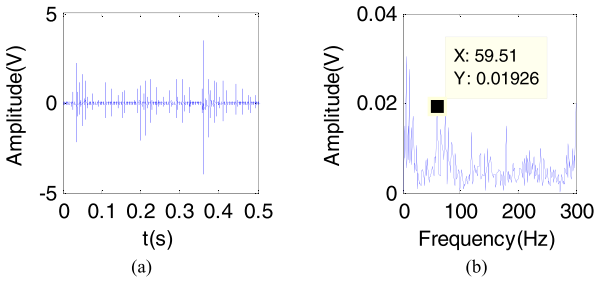

FIGURE 9. The vibration signal of compound fault at 900 rpm: (a) The waveform of signal; (b) The envelope spectrum of signal.

bearing is not in normal condition. It is easy to see that the frequency at 59.51 Hz is obvious from the spectrum diagram, indicating the outer-race fault feature can be extracted. However, the faulty bearing has another defect, which is the roller fault. Therefore, separating the roller feature from the original signal is the key to our research. To effectively separate the compound fault, the proposed method is used according the flowchart presented in the Fig. 3.

First, we use the vibration signal collected by the experimental equipment as the research object. In the actual ICD decomposition process, excessive PCs can easily lead to energy dispersion, which is not conducive to the extraction of fault features. OICD method is utilized to determine the quantity of PCs according to the technical route mentioned in the Fig. 3, and the row quantity m of the matrix V and W in the LNMF can also be obtained. The parameters are $\sigma = 0.01$ and $\mu = 0.01$ in this model. The two PCs and their spectra are shown in Fig. 10. The frequency 59.51 Hz and its double frequency (120.5 Hz) are apparent, indicating the outer race is broken because the frequency is close to the characteristic frequency of the outer race. However, the roller defect is still unable to be diagnosed. Therefore, the above-mentioned approach is used to obtain the source signal.

Second, two PCs are used to reckon the quantity of source signal. Here, potential function is utilized to determine the quantity information buried in the mixtures. Fig. 11 presents the potential function $\Phi(\theta, \lambda)$ of mixtures, indicating that the quantity of sources is two based on the two peak points existed in the curve. In this step, the columns quantity r of W and H has been obtained. Ultimately, the source signal can be separated from the PCs and the result are included in the matrix H. The separation signals based on the proposed approach are shown in Fig. 12. It is obvious that the frequency 73.2 Hz is clear, demonstrating another diagnosed fault-roller defect since the peak value is close to the theoretical result.

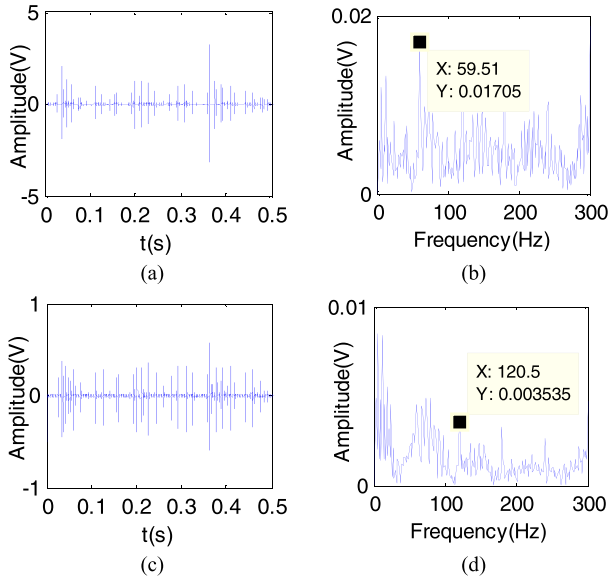

FIGURE 10. The waveform and spectra of two PCs at 900 rpm: (a) The waveform of the first PC: (b) The envelope spectrum of the first PC; (c) The waveform of the second PC; (d) The envelope spectrum of the second PC.

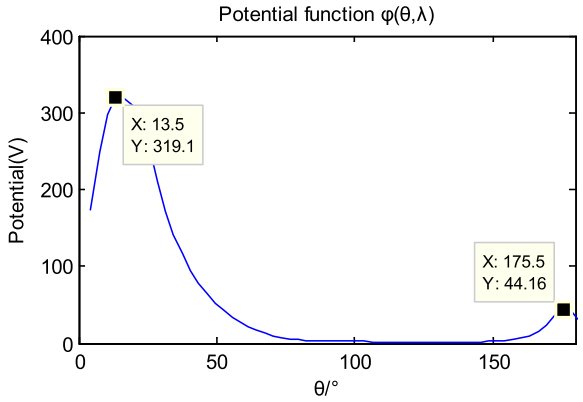

FIGURE 11. The potential function $\Phi(\theta, \lambda)$ of mixtures.

Theoretically, a series of spectral lines will be centered on the roller fault characteristic frequency f_b and its doubling frequency. Meanwhile, the center has the largest amplitude and modulation sidebands exist in the two sides of the center. In addition, the interval is equal to the cage frequency f_c. The result shown in Fig. 12(b) is consistent with the description mentioned above, indicating that the characteristic frequency is consistent with the characteristics of the rollers failure. The results indicate that the two original source signals are separated, proving the effectiveness of the proposed method.

C. COMPARATIVE TRIAL

To prove the advantage of the proposed method, the EMD-based ICA approach is utilized as an example to obtain the separation signal. Two IMFs are chosen on the same condition of the cross-correlation coefficient. The components are then used as the input matrix of ICA. The spectra of the

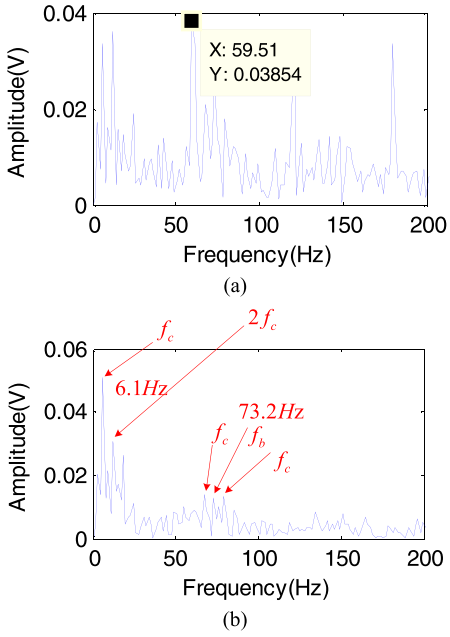

FIGURE 12. Separated source signals at 900 rpm: (a) envelope spectrum of outer-race fault; (b) envelope spectrum of roller fault.

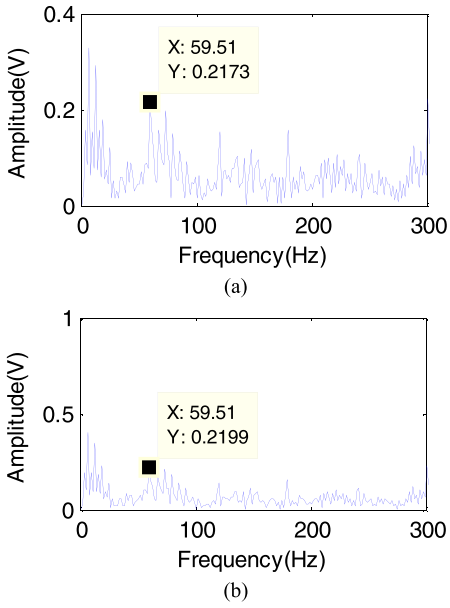

FIGURE 13. The separation signal based on the EMD-ICA method: (a) The envelope spectrum of first component; (b) The envelope spectrum of second component.

separation are presented in Fig. 13. It is apparent that only the outer-race defect feature can be extracted while the feature of roller flaw is still buried. Therefore, the EMD-based ICA method cannot perform well in compound faults diagnosis. In addition, to indicate the high efficiency of the proposed method, calculating time of the EMD method and EEMD method are added in Table 3. The result shows that the proposed method can save much more time than the other two methods.

TABLE 3. The consuming time of the two methods.

Method	EEMD	EMD	OICD
Time	512.8s	17.76s	1.47s

V. CONCLUSION

In this paper, a novel blind source separation method that combines OICD with LNMF is proposed to separate multi-faults. OICD is utilized to expand the channel when the sensors are fewer, which addresses the insufficient quantity of sensors. In the process of ICD, the CEF and EI are introduced to optimize the ICD algorithm, addressing the problem of the decomposition condition being less than ideal. The PCs are then used as the input matrix of the LNMF algorithm to separate multi-faults and the quantity of PCs is also the rows number m of matrix V in the LNMF. To estimate the quantity of sources, potential function is utilized to determine the source number which can also fix the rows quantity r of matrix H in LNMF. Finally, the separations of the multiple faults are obtained through the suggested technique. The experimental results support the effectiveness of the suggested approach. In addition, compared with the traditional ICA method —- such as EMD-based on ICA method and EEMD-based on ICA method —- the experimental results show that the proposed method successfully extracts compound fault features and saves time.

Although the method proposed in this paper can effectively separate the multiple faults, some deficiencies still exist. For example, the selection principle of PC components is not very intelligent. Therefore, future work will focus on these points to improve the performance of separating multiple faults.

REFERENCES

[1] H. Zhou, J. Chen, G. Dong, H. Wang, and H. Yuan, "Bearing fault recognition method based on neighbourhood component analysis and coupled hidden Markov model," *Mech. Syst. Signal Process.*, vols. 66–67, pp. 568–581, Jan. 2016.
[2] L. Cui, J. Huang, and F. Zhang, "Quantitative and localization diagnosis of a defective ball bearing based on vertical–horizontal synchronization signal analysis," *IEEE Trans. Ind. Electron.*, vol. 64, no. 11, pp. 8695–8706, Nov. 2017.
[3] R. B. Randall and J. Antoni, "Rolling element bearing diagnostics—A tutorial," *Mech. Syst. Signal Process.*, vol. 25, pp. 485–520, Feb. 2011.
[4] X. Yan, M. Jia, and L. Xiang, "Compound fault diagnosis of rotating machinery based on OVMD and a 1.5-dimension envelope spectrum," *Meas. Sci. Technol.*, vol. 27, no. 7, p. 075002, 2016.
[5] M. Zhang, X. Li, and J. Peng, "Using joint generalized eigenvectors of a set of covariance matrix pencils for deflationary blind source extraction," *IEEE Trans. Signal Process.*, vol. 66, no. 11, pp. 2892–2904, Jan. 2018.
[6] Y. Hao, L. Song, L. Cui, and H. Wang, "A three-dimensional geometric features-based SCA algorithm for compound faults diagnosis," *Measurement*, vol. 134, pp. 480–491, Feb. 2019.
[7] H. Zhang, X. Chen, Z. Du, X. Li, and R. Yan, "Nonlocal sparse model with adaptive structural clustering for feature extraction of aero-engine bearings," *J. Sound Vib.*, vol. 368, pp. 223–248, Apr. 2016.
[8] L. Cui, X. Gong, J. Zhang, and H. Wang, "Double-dictionary matching pursuit for fault extent evaluation of rolling bearing based on the Lempel-Ziv complexity," *J. Sound Vib.*, vol. 385, pp. 372–388, Dec. 2016.
[9] L. Song, P. Chen, and H. Wang, "Vibration-based intelligent fault diagnosis for roller bearings in low-speed rotating machinery," *IEEE Trans. Instrum. Meas.*, vol. 67, no. 8, pp. 1887–1899, Aug. 2018.
[10] L. Song, H. Wang, and P. Chen, "Step-by-step fuzzy diagnosis method for equipment based on symptom extraction and trivalent logic fuzzy diagnosis theory," *IEEE Trans. Fuzzy Syst.*, vol. 26, no. 6, pp. 3467–3478, Dec. 2018.
[11] M. S. Islam, S. Cho, and U. Chong, "Maximizing incipient fault signatures of rotating machines using wavelet entropy and cyclic logarithmic envelope spectrum," *IETE Tech. Rev.*, vol. 34, no. 3, pp. 265–275, May 2016.
[12] Z. Yan, T. Tao, Z. Jiang, and H. Wang, "Discrete frequency slice wavelet transform," *Mech. Syst. Signal Process.*, vol. 96, pp. 385–392, Nov. 2017.
[13] M. Boussé, O. Debals, and L. De Lathauwer, "A tensor-based method for large-scale blind source separation using segmentation," *IEEE Trans. Signal Process.*, vol. 65, no. 2, pp. 346–358, Jan. 2017.
[14] C. Jutten and J. Herault, "Blind separation of sources, part I: An adaptive algorithm based on neuromimetic architecture," *Signal Process.*, vol. 24, no. 1, pp. 1–10, 1991.
[15] Y.-S. Yang, A.-B. Ming, Y.-Y. Zhang, and Y.-S. Zhu, "Discriminative non-negative matrix factorization (DNMF) and its application to the fault diagnosis of diesel engine," *Mech. Syst. Signal Process.*, vol. 95, pp. 158–171, Oct. 2017.
[16] P. Spurek, J. Tabor, P. Rola, and M. Ociepka. (2017). "ICA based on the data asymmetry." [Online]. Available: https://arxiv.org/abs/1701.09160
[17] F. Wang and D. Zhao, "EMD based on independent component analysis and its application in machinery fault diagnosis," *J. Comput.*, vol. 6, no. 7, pp. 1302–1306, 2011.
[18] F. Amini and Y. Hedayati, "Underdetermined blind modal identification of structures by earthquake and ambient vibration measurements via sparse component analysis," *J. Sound Vib.*, vol. 366, pp. 117–132, Mar. 2016.
[19] X. Xu, M. Zhong, and C. Guo, "A hyperplane clustering algorithm for estimating the mixing matrix in sparse component analysis," *Neural Process. Lett.*, vol. 47, no. 2, pp. 475–490, 2017.
[20] J. Xie, P. K. Douglas, Y. N. Wu, A. L. Brody, and A. E. Anderson, "Decoding the encoding of functional brain networks: An fMRI classification comparison of non-negative matrix factorization (NMF), independent component analysis (ICA), and sparse coding algorithms," *J. Neurosci. Methods*, vol. 282, no. 17, pp. 81–94, 2017.
[21] S. Abdali and B. Nasersharif, "Non-negative matrix factorization for speech/music separation using source dependent decomposition rank, temporal continuity term and filtering," *Biomed. Signal Process. Control*, vol. 36, pp. 168–175, Jul. 2017.
[22] S. Mirzaei, H. Van Hamme, and Y. Norouzi, "Under-determined reverberant audio source separation using Bayesian non-negative matrix factorization," *Speech Commun.*, vol. 81, pp. 129–137, Jul. 2016.
[23] F. J. Canadas-Quesada, N. Ruiz-Reyes, J. Carabias-Orti, P. Vera-Candeas, and J. Fuertes-Garcia, "A non-negative matrix factorization approach based on spectro-temporal clustering to extract heart sounds," *Appl. Acoust.*, vol. 125, pp. 7–19, Oct. 2017.
[24] J. Chang, W. Liu, H. Hu, and S. Nagarajaiah, "Improved independent component analysis based modal identification of higher damping structures," *Measurement*, vol. 88, pp. 402–416, Jun. 2016.
[25] J. Wang, R. X. Gao, and R. Yan, "Integration of EEMD and ICA for wind turbine gearbox diagnosis," *Wind Energy*, vol. 17, no. 5, pp. 757–773, May 2014.
[26] H. Wang, R. Li, G. Tang, H. Yuan, Q. Zhao, and X. Cao, "A compound fault diagnosis for rolling bearings method based on blind source separation and ensemble empirical mode decomposition," *PLoS One*, vol. 9, no. 10, pp. 1–13, 2014.
[27] Y. Hao, L. Song, Y. Ke, H. Wang, and P. Chen, "Diagnosis of compound fault using sparsity promoted-based sparse component analysis," *Sensors*, vol. 17, no. 6, pp. 1307-1–1307-16, Jun. 2017.
[28] Y. Li, X. Liang, M. Xu, and W. Huang, "Early fault feature extraction of rolling bearing based on ICD and tunable Q-factor wavelet transform," *Mech. Syst. Signal Process.*, vol. 86, pp. 204–223, Mar. 2017.

YANSONG HAO was born in China, in 1992. He received the B.S. degree from the College of Mechanical and Electrical Engineering, Beijing University of Chemical Technology, China, in 2015, where he is currently pursuing the Ph.D. degree. His current research interests include fault diagnosis for rotating machinery and blind source separation.

LIUYANG SONG received the Ph.D. degree from Mie University, Japan, in 2017. She is currently involved in the Postdoctoral research at the College of Mechanical and Electrical Engineering, Beijing University of Chemical Technology, China. She is also a Temporary Researcher with the Graduate School of Environmental Science and Technology, Mie University. Her current research interests include equipment fault diagnosis technology, signal processing, and machinery inspection robot.

MENGYANG WANG was born in China, in 1992. He received the B.S. degree from the College of Mechanical and Electrical Engineering, Beijing University of Chemical Technology, China, in 2016, where he is currently pursuing the M.S. degree. His research interests include fault diagnosis for rotating machinery and blind source separation.

LINGLI CUI received the B.S. degree in mechanical engineering from Shenyang Aerospace University, Shenyang, China, in 1998, the M.S. degree in mechanical engineering and automation from the Harbin Institute of Technology, Harbin, China, in 2001, and the Ph.D. degree in control theory and control engineering from the Institute of Automation, Chinese Academy of Sciences, Beijing, China, in 2004. She is currently a Professor of mechanical engineering with the Beijing University of Technology, Beijing. Her research interests include fault mechanisms, pattern recognition, intelligent diagnosis, and fault diagnosis.

HUAQING WANG received the B.S. and M.S. degrees from the College of Mechanical and Electrical Engineering, Beijing University of Chemical Technology, China, in 1995 and 2002, respectively, and the Ph.D. degree from Mie University, Japan, in 2009. He is currently a Professor with the College of Mechanical and Electrical Engineering, Beijing University of Chemical Technology. His research interests include intelligent diagnostics for plant machinery and signal processing.